

Blast noise propagation above a snow cover

Donald G. Albert^{a)}

U.S. Army Cold Regions Research and Engineering Laboratory (USACRREL), 72 Lyme Road, Hanover, New Hampshire 03755

Lars R. Hole^{b)}

Norwegian Defence Construction Service, FBT/S, Oslo mil/Akerhus, 0015 Oslo, Norway

(Received 9 October 1998; revised 9 January 2001; accepted 8 February 2001)

A porous medium model of a snow cover, rather than a viscoelastic treatment, has been used to simulate measured, horizontally traveling acoustic waveform propagation above a dry snow cover 11–20 cm thick. The waveforms were produced by explosions of 1-kg charges at propagation distances of 100 to 1400 m. These waveforms, with a peak frequency around 30 Hz, show pulse broadening effects similar to those previously seen for higher-frequency waves over shorter propagation distances. A rigid-ice-frame porous medium (“rigid-porous”) impedance model, which includes the effect of the pores within the snow but ignores any induced motion of the ice particles, is shown to produce much better agreement with the measured waveforms compared with a viscoelastic solid treatment of the snow cover. From the acoustic waveform modeling, the predicted average snow cover depth of 18 cm and effective flow resistivities of 16–31 kPa s m⁻² agree with snow pit observations and with previous acoustic measurements over snow. For propagation in the upwind direction, the pulse broadening caused by the snow cover interaction is lessened, but the overall amplitude decay is greater because of refraction of the blast waves. © 2001 Acoustical Society of America. [DOI: 10.1121/1.1360240]

PACS numbers: 43.28.En, 43.28.Fp, 43.50.Pn, 43.50.Vt [LCS]

I. INTRODUCTION

Military training activities and firing ranges can produce loud sounds that cause significant annoyance to civilian populations. To minimize this annoyance, noise prediction models are often used to schedule military activities during periods when atmospheric and other environmental conditions are favorable. However, a better understanding of environmental effects on sound propagation and predictive models capable of including these effects are still needed.

A series of blast noise measurements has been conducted in Norway to investigate the effects of forest vegetation, micro-meteorological conditions, and winter ground conditions, and their temporal variations, on the propagation of low-frequency impulse noise. The goal of these measurements was to elucidate these environmental effects and to provide data suitable for validating more realistic propagation models.¹ In an earlier analysis of some of the Norwegian experimental data, Hole² used a Fast Field Program³ with a viscoelastic ground to predict pulses for propagation distances up to 1400 m. Predictions of overpressure amplitudes correlated well with experimental data in strongly upward and downward refracting atmospheres when a wet, slushy snow surface was present. However, the predicted amplitudes and waveforms did not agree with the measured results when a dry snow cover was present. In this paper, we analyze a subset of these measurements to examine the effect of a snow cover on the blast waves. Our purpose here is to determine whether a rigid-porous model of the snow can

predict the measured waveforms better than does the viscoelastic model.

Many authors have predicted blast overpressure as a function of distance from the source,^{4,5} but there have been fewer predictions of the entire waveform.^{6–9} Albert and Orcutt¹⁰ compared predictions and measured waveforms for short range propagation above a snow cover, and showed that the rigid-frame porous model of Attenborough¹¹ (and its low-frequency approximation) gave good agreement with the large waveform changes that were observed. Subsequently, the Attenborough model has been applied¹² to similar measurement data in an inversion process to find the snow parameters that control the acoustic effects of the snow cover. This paper applies Attenborough’s “rigid-porous” ground impedance model to predict waveforms at much longer distances and lower frequencies than were previously examined.

In the next section, we describe the measurements and the experimental data. This is followed by a brief outline of the theory of acoustic pulse propagation above a rigid-porous medium and the waveform inversion method used to determine the snow parameters. The results of these theoretical calculations are compared with the measurements, and conclusions are presented in the following sections.

II. FIELD EXPERIMENT

A. Description of site

Acoustic measurements were obtained on 22 February 1995 in an open field of pastureland at a site about 200 km north of Oslo, Norway. Two measurement locations near the north and south ends of the field were instrumented with microphones. C4 explosive charges were detonated at vari-

^{a)}Electronic mail: dalbert@crrel.usace.army.mil

^{b)}Now at: Norwegian Defense Research Establishment (NDRE), P.O. Box 25, N-2027 Kjeller, Norway; electronic mail: lrh@ffi.no

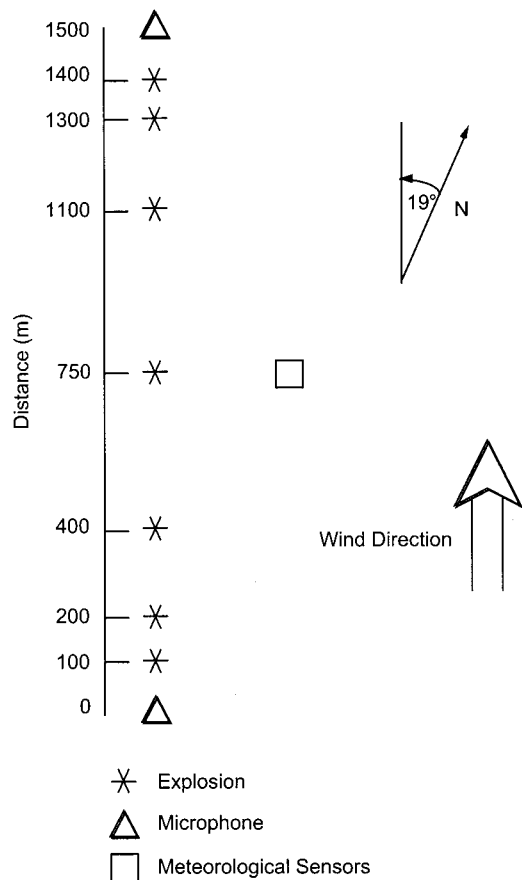


FIG. 1. Plan view of the experimental layout. The orientation of the sensor line is 341° true. Detonation height was 2 m, and the acoustic waveforms were recorded using surface microphones at the 0 (south, or upwind) and 1500 m (north, or downwind) locations.

ous distances between these measurement locations and digitally recorded (Fig. 1). The field was virtually flat, with a dry snow cover about 0.1 to 0.2 m deep. Below the snow, there was a frozen crust of soil, 0.5 m thick, which had very high compressional wave speeds (around 3000 m s^{-1}),¹³ and a density of 2100 kg m^{-3} . Apart from this thin frozen layer, conditions were *superseismic*; i.e., air pressure waves traveled faster than seismic compressional body waves, which had a typical speed of 300 m s^{-1} . Below the frozen soil crust, the soil density was around 1600 kg m^{-3} .

B. Meteorological and snow conditions

Meteorological measurements were carried out using tower-mounted instruments and a tethered balloon.¹⁴ During the acoustic measurements, the average wind speed at 10 m above ground was around 5 m s^{-1} , blowing approximately from the south toward the north, so the south location recorded waveforms that had propagated upwind, while the north location recorded waveforms that had propagated downwind. The air temperature was around 0°C . The atmospheric sound velocity profile was almost constant with time and height during the acoustic measurements. However, because of the influence of the wind, the value of the sound velocity was 326 m s^{-1} in the upwind direction (toward the south) and 336 m s^{-1} in the downwind direction (toward the

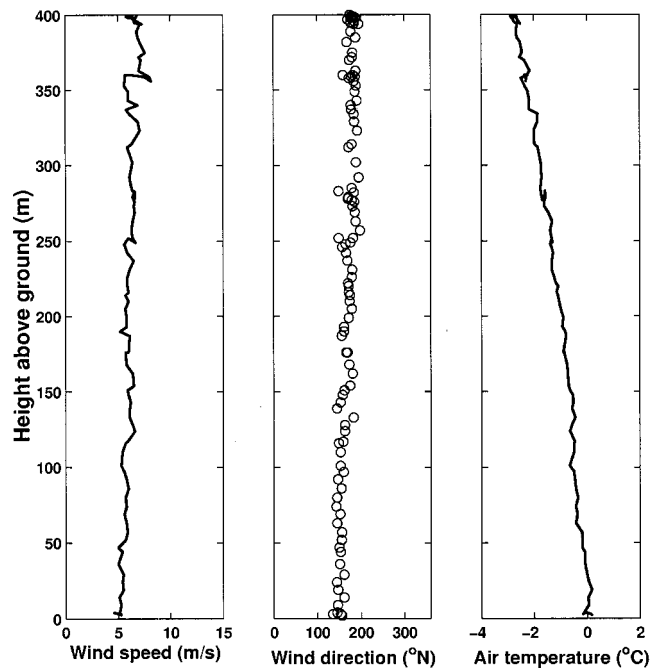


FIG. 2. Meteorological conditions during the blast noise measurements, 22 February 1252–1308 UTC, measured by Tethersonde (Ref. 19). The wind speed was approximately $4\text{--}5 \text{ m s}^{-1}$ during the tests, and always blowing approximately from the south along the detonation line.

north) in Fig. 1. Figure 2 shows the meteorological conditions during the acoustic measurements. Even though the wind profiles are almost constant with height, the wind shear close to the ground (which is not visible in Fig. 2) caused a difference in propagation conditions for the two directions studied. This will be described in Sec. IV.

Observations were made in two snow pits, concurrent with the blast noise measurements.^{15,16} The total snow cover thicknesses in the two pits were 18 and 16 cm. A hard snow layer just above the ground surface was overlain by an ice crust, and topped by a layer of newly fallen, partially broken precipitation grains. The top layer was 5–6 cm thick, with small grain sizes between 0.5 and 1 mm and a relatively low density of 125 kg m^{-3} . Beneath this layer was a permeable ice crust 1 cm thick. The lowest snow layer was 9–10 cm thick with a density of $300\text{--}350 \text{ kg m}^{-3}$. The grain size in this layer ranged from 1 to 4 mm, with rounded clusters and mixed faceted grain types, indicating that some metamorphosis was occurring. Beneath the snow and just above the soil surface was a discontinuous ice layer at the bottom 1–2 cm thick. Snow cover depths measured at other locations in the field on the day of the blast tests ranged from 11 to 20.5 cm, with most values between 14 and 16 cm.

C. Acoustical measurements

The Department of Applied Acoustics, University of Salford, England, carried out the acoustical measurements. We analyze only the acoustical data recorded using microphones placed at the snow surface. Table I contains a description of acoustical instrumentation used at both locations. (While the original data were recorded with a 20-kHz bandwidth, the data analysis discussed later was conducted after reducing the sampling rate to 2 kHz.) The reader is referred

TABLE I. Acoustical instrumentation for each measurement location. Only one channel, at 0 m height, was used in this paper.

Microphones	4 B&K, 4147
Preamplifiers	4 B&K, 2639
Recorders	SONY PC 204 4-channel DAT
Analyzers	2 Oni Sokki
Bandwidth	0.6–20 000 Hz
Microphone heights	0, 2, 4, and 8 m

to papers in the Inter-noise'96 proceedings^{1,17–21} and in a special issue of the Noise Control Engineering Journal for further details on all these measurements.^{14,15,22–24}

The experimental geometry is presented in Fig. 1. One kg charges of C4 explosive^{2,25,26} were detonated 2 m above the surface along a line between the two acoustic measurement stations, which were 1500 m apart. The blast waveforms for the downwind and upwind locations are shown in Fig. 3. For both recording locations, the duration of the waveforms increases as the propagation distance increases, and the peak amplitude decreases with distance. The amplitude decay is caused in part by spherical spreading of the blast wave front, and in part by environmental effects, as will be discussed below. The measured pulses have a broad frequency content from about 10 to 100 Hz. For the source, the central frequency for the 1-kg C4 detonations used here is around 30 Hz, compared to a peak frequency of around 200 Hz for the blank pistol shots used in previous measurements.^{10,12} For the snow surface present during these measurements, we observed that the highest frequencies

were quickly attenuated as the blast waves propagated.

The waveforms recorded at the downwind (north) location last longer than those recorded at the upwind (south) location, and they also exhibit small irregularities in their early portions that do not appear in the upwind location waveforms. Except for the shortest propagation distance (100 m), the north location waveforms also have higher peak pressure amplitudes than those at the south location. These differences with respect to propagation direction will be discussed below.

III. THEORY

A. Pulse waveform for a rigid-porous medium and homogeneous atmosphere

Although a method of calculating pulse shapes based on an empirical model of ground impedance²⁷ has been developed^{6–8,28} and works well for grass-covered ground, we have included a more complicated, but physically based, model of ground impedance in our calculations to give better agreement with observed measurements for snow.¹⁰ This model gives increased accuracy at low frequencies compared to the empirical model. We briefly outline the procedure for calculating theoretical acoustic pulse waveforms from a known (or assumed) surface. For a monofrequency source (with frequency ω) in the air and a receiver on the surface, the acoustic pressure P at a slant distance r away from the source is given by

$$\frac{P}{P_0} = \frac{e^{ikr}}{r} (1 + Q) e^{-i\omega t}, \quad (1)$$

where P_0 is a reference source pressure, k is the wave number in air, and Q is the image source strength representing the effect of the ground. At high frequencies ($kr \gg 1$), Q can be written as^{29–33}

$$Q = R_p + (1 - R_p)F(w), \quad (2)$$

where R_p is the plane wave reflection coefficient, F is the boundary loss factor, and w is a numerical distance, all of which depend on the specific impedance $Z(\omega)$ of the ground. By determining the image source strength Q_n at the n th frequency f_n , the corresponding response amplitude \hat{P}_n can be written as:

$$\hat{P}_n = \frac{P_0}{4\pi r} S_n W_n (1 + Q_n) e^{i2\pi f_n r/c}, \quad n=0,1,2,\dots,N-1, \quad (3)$$

where S_n and W_n represent the source and instrument effects at the n th frequency and c is the speed of sound in air. An inverse FFT,

$$P_m = \frac{1}{N} \sum_{n=0}^{N-1} \hat{P}_n e^{-i2\pi mn/N}, \quad m=0,1,2,\dots,N-1, \quad (4)$$

is used to construct theoretical pulse waveforms in the time domain. An explicitly layered model of the ground must be used to represent thin snow covers³⁴ using (omitting the frequency subscripts)

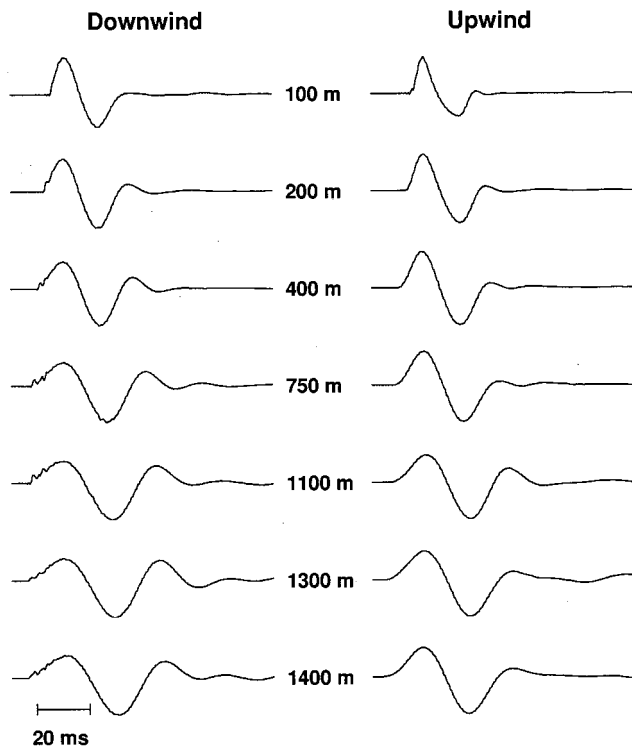


FIG. 3. Normalized blast waveforms experimentally observed by surface microphones for 1-kg explosive charges detonated 2 m above the surface. Although the propagation distances are the same for both observation locations, the waveforms recorded at the downwind location are longer than those measured at the upwind location.

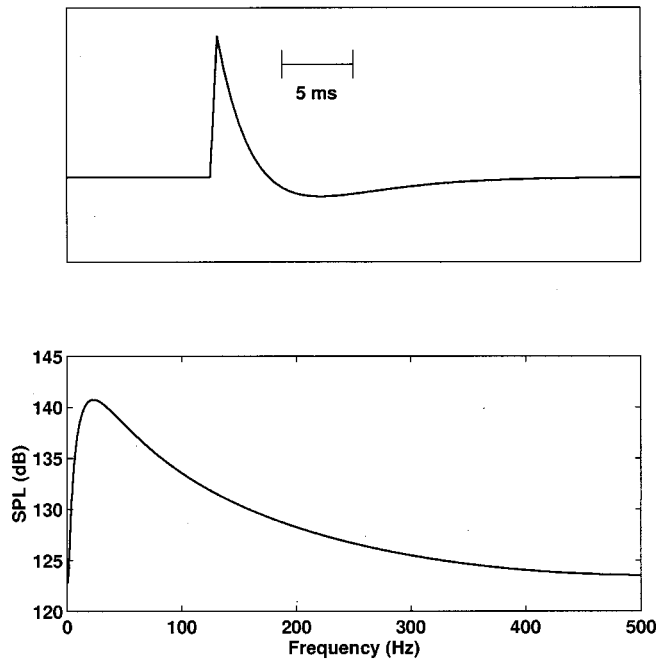


FIG. 4. Assumed source waveform (a) and its power spectrum (b) used in the theoretical calculations.

$$Z = Z_2 \frac{Z_3 - iZ_2 \tan k_2 d}{Z_2 - iZ_3 \tan k_2 d}, \quad (5)$$

where d is the snow layer thickness, k_2 is the wave number in the snow layer, and Z_2 and Z_3 are the impedances of the snow layer and substratum, respectively.³⁵

The acoustic behavior of the soil or snow is specified by the impedance Z_2 and wave number k_2 , which are used in Eqs. (5) and (2) to find the theoretical waveform. We use Attenborough's four-parameter model of ground impedance¹¹ to calculate these parameters. The four input parameters are the effective flow resistivity σ , the porosity Ω , the pore shape factor ratio s_f , and the grain shape factor n' . The snow depth d and the substrate properties are also required in a layered model.

An exponentially decaying source pulse $S(t)$ of the form

$$S(t) = P^+ (1 - t/t_+) e^{-t/t_+} \quad (6)$$

is used as the starting waveform in all of the blast wave calculations. In Eq. (6), P^+ is the positive peak overpressure, t the time, and t_+ the duration of the positive overpressure. This pulse shape is sometimes known as a Friedlander waveform, and has been previously used in blast wave calculations^{25,36,37} and in the ANSI standard blast noise estimation method.³⁸ Values of $P^+ = 55$ kPa and $t_+ = 3.6$ ms were selected to represent the blast wave produced by a 1-kg charge of C4 at a distance of 5 m,²⁵ and all calculations began with this source pulse. The waveform and spectrum of the source are shown in Fig. 4.

B. Inversion technique

The acoustic pulse calculation method discussed in the previous section can be used to calculate the pulse shape for a C4 blast if the geometry (source and receiver heights and

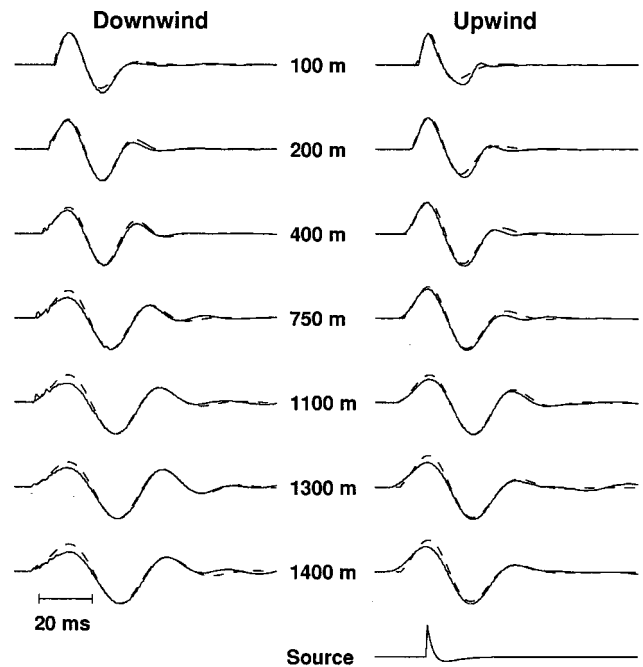


FIG. 5. Observed (solid line) and predicted (dashed line) waveforms at the snow surface, made using the rigid-porous medium model, for the downwind and upwind measurement locations. The source waveform used to calculate the predicted waveforms appears at the bottom of the figure.

propagation distance) and ground properties (parameters needed for Attenborough's rigid-porous ground impedance model) are known. The calculation method assumes that the atmosphere is homogeneous. The method can also be used in a waveform inversion procedure to estimate the unknown ground parameters that produce a measured waveform. In this procedure, the geometry and some of the ground parameters (discussed below) are known and are fixed at a constant value in the inversion calculations. Pulses are calculated using Eqs. (1)–(6) using assumed starting values of the unknown parameters, and the calculated waveforms are directly compared with the observed waveforms.¹² The unknown parameters are varied in a systematic way using an iterative search procedure³⁹ until good agreement is obtained.

For our rigid-porous medium calculations, the grain shape factor n' was set to 0.5, corresponding to spherical grains, and the porosity $\Omega = 0.70$ was determined from the measured average density, 275 kg m^{-3} , of the entire snow cover. We fixed the pore shape factor ratio s_f at 0.8 for dry snow.¹² Parameters for the frozen soil¹² beneath the snow were fixed at $\sigma = 3000 \text{ kPa s m}^{-2}$, $\Omega = 0.27$, $s_f = 0.73$, and $n' = 0.5$. Only the effective flow resistivity σ of the snow and the snow depth d were varied in the inversion procedure.

Waveform inversion to determine the snow parameters was performed independently for each source–receiver distance. We compared calculated and observed pulses using time-aligned, normalized waveforms.

IV. RESULTS

The measured and automatically calculated waveforms are compared in Fig. 5, and the snow parameters determined from the inversion procedure are listed in Table II. In general

TABLE II. Waveform inversion results.

Range (m)	Downwind location		Upwind location	
	Effective flow resistivity (σ) kPa s m ⁻²	Snow depth (cm)	Effective flow resistivity (σ) kPa s m ⁻²	Snow depth (cm)
100	21	25	57	19
200	16	21	34	19
400	20	17	37	17
750	28	18	51	15
1100	29	18	37	15
1300	24	17	58	15
1400	31	18	72	14

there is good agreement, and the theoretical waveforms match the measured waveform shapes and time duration. These calculations show that a model with a rigid-porous ground surface and a homogeneous atmosphere is sufficient to explain the waveform elongation in the measured data.

Figure 6 compares the experimentally measured waveform for the downwind measurement location with the rigid-porous snow cover calculations of this paper and with a Fast Field Program (FFP) calculation, assuming a viscoelastic ground surface, that did not take the dry snow cover into account.² The propagation distance was 1300 m. The improvement in the modeling accuracy using the porous treatment of the snow is clear from this figure. Previous modeling calculations^{2,40} have shown that no selection of parameters for a viscoelastic model will be able to produce the correct amount of waveform broadening shown by the measured data.

The snow cover depths determined by the theoretical

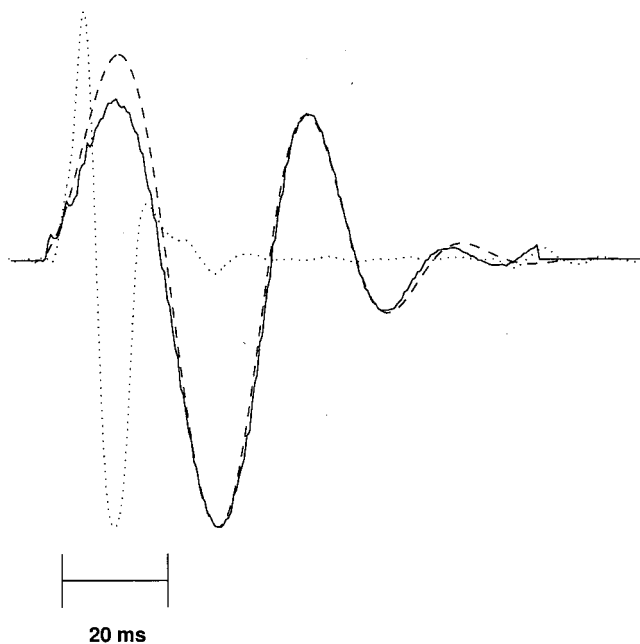


FIG. 6. Comparison of the experimental waveform (solid line) at downwind (north) measurement location, 1300 m from the source with a Fast Field Program (FFP) calculation using a viscoelastic ground (dashed line, same result as in Fig. 9 in Hole, Ref. 2), and with the rigid-porous medium calculations of this paper (dotted line). All waveforms have been normalized.

waveform inversions have an average value of 18 ± 3 cm, in agreement with the measured snow depths of 16 and 18 cm at two widely spaced snow pits. The effective flow resistivities derived from the inversion are nearly constant for the north downwind location, ranging between 16 and 31 kPa s m⁻². For the upwind location, the values are higher, 34–72 kPa s m⁻², and they seem to fluctuate randomly with distance.

These results can be explained by the effects of the snow cover and the wind. For the downwind location, the blast waves tended to be refracted downward causing them to interact strongly with the porous snow. While the refraction by the wind tends to increase the wave amplitude, compared with the case of a homogeneous atmosphere, the interaction with the snow decreased the amplitude and elongated the waveform. This pulse broadening leads to a low effective flow resistivity in the inversion process. The inversion results are constant with increasing propagation distance, as expected from the fairly uniform snow cover.

The pulse broadening observed at the upwind location was less than at the downwind location, so the effective flow resistivities determined by the waveform inversion procedure are higher. Here, the propagation was upwind, so that the waves tended to be refracted upward, away from the snow surface. Although these waves interacted less with the snow cover, they have lower peak pressure amplitudes because some of the energy that was refracted upward never reaches the microphone on the ground. The amplitudes, and the inversion parameters, fluctuate more than for the downwind waveforms because they are strongly affected by slight fluctuations in the wind. The waveform and amplitude changes in this case are caused by both the wind-generated refraction and by snow cover interaction.

Single frequency Fast Field Program calculations presented in Fig. 7 demonstrate the effect of the wind shear close to the ground. A viscoelastic ground surface with a compressional wave velocity of 1500 m s⁻¹, shear wave velocity of 1000 m s⁻¹, and density of 2000 kg m⁻³ was used in the calculations. The refractive effect of the wind shear for a speed of 5 m s⁻¹ at 10 m height above the ground (Fig. 2) was modeled first by setting the sound velocity in the calculations to 331 m s⁻¹ at the ground. Then the sound velocity was smoothly varied to values of 336 m s⁻¹ for the downwind case and 326 m s⁻¹ for the upwind case.

The solid lines in Fig. 7 show the calculated difference in transmission loss between the upwind and downwind directions at 30, 50, and 100 Hz, and clearly demonstrate the expected wind effect at these low frequencies. The circles in Fig. 7 show the measured differences in the peak amplitudes for the blast wave pulses. These measured (broadband) differences are similar to the calculated values at 30 Hz corresponding to the peak pulse frequencies. This figure shows that the differences between the measured amplitudes in the upwind and downwind directions can be attributed to the wind effects.

The effective flow resistivities, 16–31 kPa s m⁻², determined for the snow cover for downwind propagation agree with values determined from most previous pulse measurements on seasonal snow.^{12,15,21}

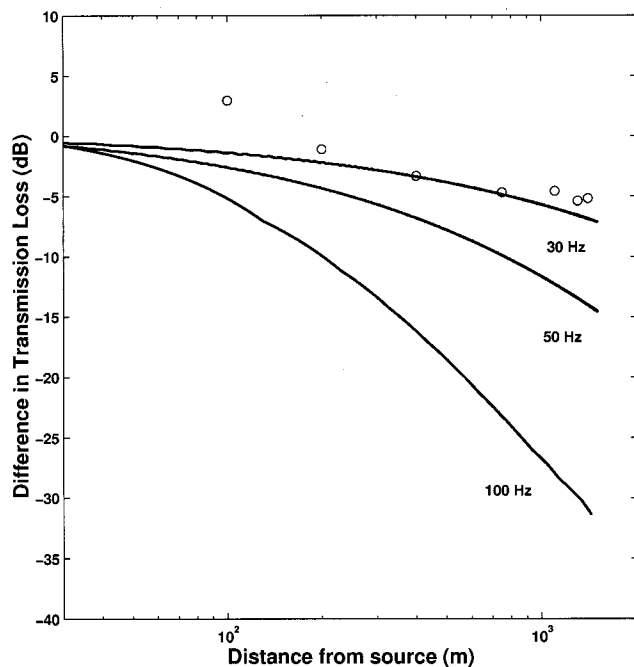


FIG. 7. Measured and calculated amplitude differences between upwind and downwind propagation directions. The measured differences in peak amplitudes are shown by circles. The theoretical differences (solid lines) were calculated using a single frequency FFP with a viscoelastic ground surface and a wind speed of 5 m s^{-1} at 10 m height.

Impedance tube measurements⁴¹ done the day after the blast measurements gave relatively high values for the effective flow resistivity of $59\text{--}69 \text{ kPa s m}^{-2}$. However, rain had fallen on the snow after the blast noise measurements, and the warm air temperature overnight may have caused substantial changes in the snow structure by the time the impedance tube measurements were conducted.

Note that in both the downwind and upwind cases, the waveform inversion method uses a homogeneous atmosphere and therefore attributes all of the observed waveform shape changes to the snow cover properties only. There is no difference in the actual snow cover properties in the upwind and downwind directions, and the true flow resistivity should be nearly uniform. The differences in the effective flow resistivity values determined by this procedure arise from ignoring all of the atmospheric effects in the waveform inversion calculations.

V. SUMMARY AND CONCLUDING REMARKS

Blast waves propagating in the upwind and downwind directions above a dry snow cover exhibit pulse broadening caused by wave interaction with the snow cover. By modeling the effect of the snow cover using a rigid-frame porous medium model, the predicted pulse shapes are in much better agreement with experimental results than are previously published calculations using a Fast Field Program with a viscoelastic ground surface that did not take the dry snow cover into account. These results indicate that a porous boundary condition is required for correctly modeled sound propagation over snow.

Note added in proof: A database of the experimental measurements from the Norwegian trials is available from the second author. Additional analysis of the Norwegian data appears in Ref. 42.

ACKNOWLEDGMENTS

We thank Robert L. Guice at ARA, USA, for organizing acoustic and seismic data; Geoffrey Kerry at University of Salford, U.K., for providing the measured acoustic data; Amir M. Kaynia and Christian Madshus at NGI, Norway, for determining the seismic properties of the test site; and Steve Arcone and Mark Moran, CRREL, for technical reviews. The field experiment was initiated and managed by Arnfinn Jenssen at NDCS, Norway. We especially thank the anonymous reviewers and the Associate Editor, Lou Sutherland, for many constructive and helpful comments. This work was funded by the Norwegian Defense Construction Service and the Directorate of Research and Development, U.S. Army Corps of Engineers.

- ¹G. Kerry, "An overview of the long range impulse sound propagation measurements made in Norway," Inter-noise 96, Liverpool, UK, 583–588 (1996).
- ²L. R. Hole, "An experimental and theoretical study on propagation of acoustic pulses in a strongly refracting atmosphere," *Appl. Acoust.* **53**, 583–588 (1997).
- ³H. Schmidt, *SAFARI: Seismo-acoustic fast field algorithm for range-independent environments. User's guide*, Report SR-113 (SACLANTCEN, 1987).
- ⁴J. W. Reed, *BLASTO, a PC program for predicting positive phase overpressure at distance from an explosion* (JWR Inc., Albuquerque, NM, n.d.).
- ⁵G. Kerry, D. J. Saunders, and A. Sills, "The use of meteorological profiles to predict the peak sound pressure level at distance from small explosions," *J. Acoust. Soc. Am.* **81**, 888–896 (1987).
- ⁶R. Raspet, J. Ezell, and H. E. Bass, "Additional comments on and erratum for 'Effect of finite ground impedance on the propagation of acoustic pulses' [*J. Acoust. Soc. Am.* **74**, 267–274 (1983)];" *J. Acoust. Soc. Am.* **77**, 1955–1958 (1985).
- ⁷R. Raspet, H. E. Bass, and J. Ezell, "Effect of finite ground impedance on the propagation of acoustic pulses," *J. Acoust. Soc. Am.* **74**, 267–274 (1983).
- ⁸C. G. Don and A. J. Cramond, "Impulse propagation in a neutral atmosphere," *J. Acoust. Soc. Am.* **81**, 1341–1349 (1987).
- ⁹I. P. Chunchuzov, G. A. Bush, and S. N. Kulichov, "On acoustical impulse propagation in a moving inhomogeneous atmospheric layer," *J. Acoust. Soc. Am.* **88**, 455–461 (1990).
- ¹⁰D. G. Albert and J. A. Orcutt, "Acoustic pulse propagation above grassland and snow: Comparison of theoretical and experimental waveforms," *J. Acoust. Soc. Am.* **87**, 93–100 (1990).
- ¹¹K. Attenborough, "Acoustical impedance models for outdoor ground surfaces," *J. Sound Vib.* **99**, 521–544 (1985).
- ¹²D. G. Albert, "Acoustic waveform inversion with application to seasonal snow covers," *J. Acoust. Soc. Am.* **109**, 91–101 (2001).
- ¹³A. M. Kaynia and C. Madshus, *Blast propagation through forest-NOR 95/1 tests*, NGI report 515137-4 (Norwegian Geotechnical Institute, Oslo, Norway, 1995).
- ¹⁴L. R. Hole, Y. Gjessing, and T. de Lange, "Meteorological measurements and conditions during Norwegian trials," *Noise Control Eng. J.* **46**, 199–207 (1998).
- ¹⁵D. G. Albert, "Snow cover properties from impulsive noise propagation measurements," *Noise Control Eng. J.* **46**, 208–214 (1998).
- ¹⁶S. Bakkehoi, *Snow classification during tests at Haslemoen, February 1995*, NGI Report 515137-4 (Norwegian Geotechnical Institute, Oslo, Norway, 1995).
- ¹⁷R. Guice and A. Jenssen, "Impulse noise measurements in a forest during summer and winter—An overview of measurements," Inter-Noise 96, Liverpool, UK, 2589–2594 (1996).

- ¹⁸M. Trimpop and K.-W. Hirsch, "On the advantage of relational data structures and client/server applications for shooting noise data using ODBC, SQL and OLE standards," *Internoise 96*, Liverpool, UK, 549–554 (1996).
- ¹⁹L. R. Hole, Y. Gjessing, and T. de Lange, "Meteorological measurements during Norwegian Trials," *Inter-noise 96*, Liverpool, UK, 605–610 (1996).
- ²⁰C. Madshus and A. M. Kanyia, "Ground response to propagating airblast," *Inter-Noise 96*, Liverpool, UK, 1433–1438 (1996).
- ²¹D. G. Albert, "Snow cover effects on impulsive noise propagation in a forest," *Inter-Noise 96*, Liverpool, UK, 663–668 (1996).
- ²²K.-W. Hirsch, "On the influence of local ground reflections on sound levels from distant blasts at large distances," *Noise Control Eng. J.* **46**, 215–226 (1998).
- ²³R. L. Guice, L. R. Hole, A. Jenssen, and G. Kerry, "Impulsive noise measurements in a forest during summer and winter conditions," *Noise Control Eng. J.* **46**, 185–189 (1998).
- ²⁴C. Madshus and A. M. Kaynia, "Measurement and interpretation of ground response to airblast," *Noise Control Eng. J.* **46**, 191–198 (1998).
- ²⁵L. Kennedy, S. Hikida, and R. Ekler, *Overpressure and dynamic pressure waveforms for small C4 charge detonations*, Report No. SSS-DFR-94-14507 (Maxwell S-Cubed Division, Albuquerque, NM, 1994).
- ²⁶R. Ford, D. J. Saunders, and G. Kerry, "The acoustic pressure waveform from small unconfined charges of plastic explosive," *J. Acoust. Soc. Am.* **94**, 408–417 (1993).
- ²⁷M. E. Delaney and E. N. Bazley, "Acoustical properties of fibrous absorbent materials," *Appl. Acoust.* **3**, 105–116 (1970).
- ²⁸A. J. Cramond and C. G. Don, "Reflection of impulses as a method of determining acoustic impedance," *J. Acoust. Soc. Am.* **75**, 382–389 (1984).
- ²⁹K. Attenborough, S. I. Hayek, and J. M. Lawther, "Propagation of sound above a porous half-space," *J. Acoust. Soc. Am.* **68**, 1493–1501 (1980).
- ³⁰K. U. Ingard, "On the reflection of a spherical wave from an infinite plane," *J. Acoust. Soc. Am.* **23**, 329–335 (1951).
- ³¹I. Rudnick, "Propagation of an acoustic wave along a boundary," *J. Acoust. Soc. Am.* **19**, 348–356 (1947).
- ³²C. I. Chessell, "Propagation of noise along a finite impedance boundary," *J. Acoust. Soc. Am.* **62**, 825–834 (1977).
- ³³C. F. Chien and W. W. Soroka, "Sound propagation along an impedance plane," *J. Sound Vib.* **43**, 9–20 (1975).
- ³⁴J. Nicolas, J.-L. Berry, and G. A. Daigle, "Propagation of sound above a finite layer of snow," *J. Acoust. Soc. Am.* **77**, 67–73 (1985).
- ³⁵L. M. Brekhovskikh, *Waves in Layered Media*, 2nd ed. (Academic, New York, 1980).
- ³⁶W. E. Baker, *Explosions in Air* (University of Texas Press, Austin, 1973), p. 268.
- ³⁷M. J. Crocker and L. C. Sutherland, "Instrumentation requirements for measurement of sonic boom and blast waves—A theoretical study," *J. Sound Vib.* **7**, 351–370 (1968).
- ³⁸ANSI, "Estimating airblast characteristics for single point explosions in air, with a guide to evaluation of atmospheric propagation and effects" (American National Standards Institute, New York, 1983), p. vi+25.
- ³⁹W. H. Press, B. P. Flannery, S. A. Teukolsky, and W. T. Vetterling, *Numerical Recipes: The Art of Scientific Computing* (Cambridge University Press, New York, 1986).
- ⁴⁰D. G. Albert, *Attenuation of outdoor sound propagation levels by a snow cover*, CRREL Report 93-20 (USA CRREL, Hanover, NH, 1993).
- ⁴¹S. Storeheier, *A preliminary investigation on the acoustic characterization of snow at the Haslemoen site*, Report 40-NO950182 (Sintef Delab, Trondheim, Norway, 1995).
- ⁴²H. Dong, A. M. Kaynia, C. Madshus, and J. M. Hovem, "Sound propagation over layered poroelastic ground using a finite-difference model," *J. Acoust. Soc. Am.* **108**, 494–502 (2000).